



HHS Public Access

Author manuscript

Int J Obes (Lond). Author manuscript; available in PMC 2016 September 17.

Published in final edited form as:

Int J Obes (Lond). 2016 June ; 40(6): 921–928. doi:10.1038/ijo.2016.38.

Eating in mice with gastric bypass surgery causes exaggerated activation of brainstem anorexia circuit

Michael B. Mumphrey, Zheng Hao, R. Leigh Townsend, Laurel M. Patterson, Heike Münzberg, Christopher C. Morrison, Jianping Ye, and Hans-Rudolf Berthoud

Pennington Biomedical Research Center, Louisiana State University System, Baton Rouge, LA 70808, USA

Abstract

Background/Objective—Obesity and metabolic diseases are at an alarming level globally and increasingly affect children and adolescents. Gastric bypass and other bariatric surgeries have proven remarkably successful and are increasingly performed worldwide. Reduced desire to eat and changes in eating behavior and food choice account for most of the initial weight loss and diabetes remission after surgery, but the underlying mechanisms of altered gut-brain communication are unknown.

Subjects/Methods—To explore the potential involvement of a powerful brainstem anorexia pathway centered around the lateral parabrachial nucleus (IPBN) we measured meal-induced neuronal activation by means of c-Fos immunohistochemistry in a new high-fat diet-induced obese mouse model of Roux-en-Y gastric bypass (RYGB) at 10 and 40 days after RYGB or sham surgery.

Results—Voluntary ingestion of a meal 10 days after RYGB, but not after sham surgery, strongly and selectively activates calcitonin gene-related peptide neurons in the external IPBN as well as neurons in the nucleus tractus solitaries, area postrema, and medial amygdala. At 40 days after surgery, meal-induced activation in all these areas was greatly diminished and did not reach statistical significance.

Conclusions—The neural activation pattern and dynamics suggest a role of the brainstem anorexia pathway in the early effects of RYGB on meal size and food intake that may lead to adaptive neural and behavioral changes involved in the control of food intake and body weight at a lower level. However, selective inhibition of this pathway will be required for a more causal implication.

Keywords

Obesity; high-fat diet; parabrachial nucleus; amygdala; solitary nucleus

Users may view, print, copy, and download text and data-mine the content in such documents, for the purposes of academic research, subject always to the full Conditions of use: http://www.nature.com/authors/editorial_policies/license.html#terms

Correspondence to: Hans-Rudolf Berthoud, Pennington Biomedical Research Center, 6400 Perkins Road, Baton Rouge, LA 70808, Phone: (225) 763 2688, Fax: (225) 763 0260, berthohr@pbrc.edu.

Conflict of Interest: The authors declare no conflict of interest

Introduction

The most effective and lasting treatments currently available for obesity are bariatric surgeries such as Roux-en-Y gastric bypass (RYGB) and vertical sleeve gastrectomy (VSG). Unlike dieting, these surgeries do not elicit strong adaptive counterregulatory responses such as increased hunger and hypometabolism, which often lead to relapse. There has been intense research trying to identify the mechanisms responsible for the beneficial effects of bariatric surgeries on body weight and glycemic control in rodent models (1–11), but no clear picture has yet emerged. What all surgeries in humans and rodents have at least initially in common is anorexia, driving body weight loss and to a large part diabetes resolution (12–15). In humans, sustained reduction of food intake is a hallmark of successful surgeries and has been observed for up to 10 years post-surgery (16, 17). Recent studies in rodents have clearly demonstrated that the more effective bariatric surgeries, RYGB and VSG, do not simply restrict the total amount of food that can be ingested (18, 19), and some surgeries in humans fail because they lack suppression of food intake. Therefore, identification of the neural mechanisms responsible for keeping food intake suppressed in spite of greatly reduced body weight will be crucial in ultimately replacing surgery with more targeted approaches.

Recent studies have re-discovered the parabrachial nucleus (PBN) as an important relay station between areas of the caudal brainstem and the forebrain involved in ingestive behavior. Wu and Palmiter (20–22) have demonstrated that “unopposed” activity of the lateral parabrachial nucleus (LPBN) by removing GABA_A inhibitory input from agouti-related peptide (AgRP) neurons in the hypothalamic arcuate nucleus leads to starvation, which can be rescued by a number of manipulations of the nucleus tractus solitarius (NTS) → PBN → central amygdala (CeA) axis. This suggests that the strong feeding drive emanating from arcuate AgRP/neuropeptide Y neurons at least partly results from inhibition of an equally strong feeding inhibitory or anorexia circuit organized around the IPBN (23, 24). Neurons in the IPBN expressing calcitonin gene-related peptide (CGRP) and projecting to a sub-region of the CeA (25–27) are critical for the suppression of food intake by large doses of the gastrointestinal hormone cholecystokinin (CCK) and by substances producing gastrointestinal malaise such as lithium chloride (LiCl) (28).

Given that RYGB potently inhibits meal size and food intake both in rodents and humans (17, 29), we hypothesized that the IPBN brainstem anorexia circuit might be disproportionately activated during consummation of a meal, particularly early after surgery. We therefore assessed meal-induced neural activation by means of c-Fos immunohistochemistry in the IPBN, NTS, and CeA in mice with RYGB or sham surgery.

Materials and Methods

Animals

Male C57BL6J mice (Harlan Industries, Indianapolis, IN) were housed individually in wire-mesh cages at a constant temperature of 21–23° C with a 12h light-dark cycle (lights on 07:00, off at 19:00). Food and water were provided ad libitum unless otherwise indicated. Animals were made obese by putting them on a two-choice diet for 8 weeks consisting of

normal laboratory chow (Chow, Kcal%: Carb, 58; Fat, 13.5; Prot, 28.5, # 5001, Purina LabDiet, Richmond, IN) and high-fat diet (HF, Kcal%: Carb, 20; Fat, 60; Prot, 20, D12492, Research Diets, New Brunswick, NJ), with each of the diets containing sufficient minerals and vitamins. They were then randomly assigned to either RYGB or sham-surgery. All protocols were approved by the Institutional Animal Care and Use Committee at the Pennington Biomedical Research Center in accordance with guidelines established by the National Institutes of Health.

Roux-en-Y gastric bypass surgery

The surgical procedure has been described in detail earlier (30, 31). Briefly, in overnight food deprived mice, the small intestine was transected at the mid-jejunum and the distal end was anastomosed to a small gastric pouch, forming the Roux-limb. The proximal end of the cut jejunum was anastomosed to the lower jejunum forming the biliopancreatic limb. Sham surgery consisted of laparotomy and mobilization of stomach and small intestine or in some cases, jejunostomy and re-anastomosis. Adequate postoperative care was provided and food made available on the day after surgery, with no major problems and no mortality.

Measurement of food intake, body weight, and body composition

Food intake was measured by weighing both chow and high-fat diet separately accounting for spillage. Body weight was measured daily. Body composition was measured one day before the meal test using a Minispec LF 90 NMR Analyzer (Bruker Corporation, The Woodlands, TX).

Meal tests

At 8–12 or 38–40 days after surgery (referred to as 10 and 40 days after surgery throughout the manuscript), overnight food deprived animals were given access to a high-fat food pellet at 08:00 h – 10:00 h and ingestive behavior was monitored by an observer. In RYGB mice, latency was typically around 1 minute. After 10 min the remaining food was removed and the ingested portion calculated while accounting for spillage. Since mice with sham-surgery ate faster and consumed larger meals compared with RYGB mice, food was removed after about 5 min to roughly match intake of RYGB mice. Ninety minutes after the start of ingestion, mice were euthanized and transcardially perfused for immunohistochemistry.

Tissue preparation and immunohistochemical processing

Mice were deeply anesthetized with pentobarbital sodium (90mg/kg) and transcardially perfused with heparinized saline (20U/ml) followed by ice cold, 4% phosphate-buffered (pH 7.4) paraformaldehyde. Brains were extracted, blocked, and post-fixed in the same fixative overnight. Prior to cryosectioning, the tissue was immersed for 24 h in an 18% sucrose solution in phosphate-buffered saline (PBS) with 0.05% sodium azide. Free-floating, frozen sections of 30 μ m were cut, separated into five series, and either processed immediately or stored in cryoprotectant solution at -20°C .

Complete series of one-in-five sections stretching the entire rostrocaudal dimensions of the IPBN, NTS, and amygdala were processed for c-Fos immunohistochemistry using the ABC/NiDAB method. Briefly, the tissue was pretreated with a solution of 0.5% sodium

borohydride in PBS. Appropriate washes in PBS followed this and subsequent incubations. Incubation in the primary antibody (rabbit anti-c-Fos, AB-5, 1:10,000, Oncogene/EMD Biosciences, La Jolla, CA; or goat anti-c-Fos, 1:1,000, Santa Cruz Biotech, Dallas, TX) was for 20 h at room temperature (RT) and was followed by 2 h in a biotinylated secondary antibody (donkey anti-rabbit, 1:500, Jackson ImmunoResearch, West Grove, PA; donkey anti-goat, 1:500, Jackson ImmunoResearch). The sections were then incubated for 1 h in avidin-biotin complex (1:500; Vectastain ABC Elite Kit, Vector Labs, Burlingame, CA). The nuclear c-Fos was visualized using a blue-black metal-enhanced 3, 3'-diaminobenzidine tetrahydrochloride (NiDAB) substrate kit (Thermoscientific/Pierce, Rockford, IL).

c-Fos staining was followed by immunofluorescent labeling for CGRP or tyrosine hydroxylase (TH). Sections were reincubated with the blocking solution before incubation in the second primary antiserum (mouse anti-CGRP, 1:2500, UCLA/CURE Digestive Research Center, Los Angeles, CA; rabbit anti-TH, 1:1000, Millipore, Billerica, MA) for 20 h at RT or 40 h at 4° C. The secondary antibody (Cy3 donkey anti-mouse, 1:500, Jackson ImmunoResearch; Cy3 donkey anti-rabbit, 1:500, Jackson ImmunoResearch) was applied for 2 h at RT in the dark. Sections were mounted on charged slides using Fluoromount-G (Southern Biotech, Birmingham, AL) as the mounting medium.

Quantitative microscopic analyses

For quantitative assessment of c-Fos, 3–5 sections were selected for the NTS (from –7.20 to –7.70 mm from Bregma), PBN (from –5.02 to –5.34 mm from Bregma), and CeA (from –0.94 to –1.82 mm from Bregma) and images were generated through a X20 objective in a Zeiss Axioscope microscope. Neurons were classified as c-Fos positive according to the presence above background of black NiDAB reaction product in the cell nucleus. When double labelling for CGRP (PBN) or TH (NTS), cells were classified as positive according to the presence above background of red fluorescence in the cell cytoplasm. Doubly stained cells were considered double labelled according to the presence of both NiDAB reaction products in the cell nucleus (c-Fos) and red fluorescence in the cytoplasm (CGRP or TH).

Statistical analyses

Body composition was analyzed by two-way ANOVA with time as within subject factor and surgical group as between subject factor. Immunohistochemical cell counts were analyzed using two-way ANOVA with surgical group and meal consumption as between subject factors. All two-way ANOVAs were followed by Bonferroni-adjusted multiple comparisons. Chow preference, cumulative food intake, and test meal size were analyzed using t-tests. All data were expressed as mean \pm SEM.

Results

RYGB leads to a transient decrease in food intake and a sustained loss of body weight

As reported previously (30, 31), RYGB in mice results in sustained weight loss and transient suppression of food intake. Ten days post-surgery, body weight decreased $15.8 \pm 0.8\%$ after RYGB and $3.5 \pm 1.1\%$ after sham surgery ($p < 0.01$; Fig. 1a). Body weight after RYGB remained at a lower level with only a slight and insignificant increase from the nadir at 10–

20 days after surgery. In contrast, sham-operated mice rapidly recovered from the initial weight loss and gained $23.1 \pm 2.8\%$ from before to 38 days after surgery. Measurement of body composition at day 38 showed that weight loss of RYGB animals was fully accounted for by loss of fat but not lean mass (Fig. 1b).

Food intake following RYGB was significantly suppressed for the first 8 days and returned to levels no longer significantly different from pre-surgical or sham-operated levels 10 days after surgery (Fig. 1c). RYGB and sham-operated mice started eating significant amounts of high-fat diet one day after surgery, and no special liquid diet was necessary. There were no complications and no mortality in the entire cohort of 39 RYGB and 34 sham animals.

While total food intake was not significantly different between the two groups from days 10–40, chow preference measured over 6 days (postsurgical days 25–30) showed a significant difference between groups (Fig. 1c inset). RYGB animals chose $8.3 \pm 0.3\%$ of their daily calories from regular (low-fat) chow, almost 3 times more than the sham group which chose only $2.6 \pm 0.2\%$ of their calories from chow. However, during the first 8 days after surgery, chow preference was not different between RYGB and sham mice.

At 10, but not 40, days after RYGB, eating a voluntary meal induces exaggerated c-Fos expression in the IPBN, NTS, AP, and CeA

To assess the effects of food ingestion on neural activity, we allowed mice to consume high fat diet for 10 minutes after an overnight (16 h) fast. Importantly, test meal size for RYGB and sham mice was not significantly different within each time point and for RYGB mice tested at 10 or 40 days. However, meal size was significantly lower for RYGB mice tested at 40 days when compared to mice tested at 10 days (Fig. 2c).

Ten days after surgery, strong c-Fos expression was observed after eating a meal in the IPBN of RYGB, but not sham-operated, mice (Fig. 2a, b), and there was very little c-Fos in both groups when no meal was ingested. Meal-induced c-Fos expression was limited to the external lateral subnucleus. At 40 days after surgery, meal-induced c-Fos expression was strongly diminished in the IPBN of RYGB mice and was no longer significantly higher than sham or no meal controls (Fig. 2f). There was a strong and significant positive correlation between c-Fos expression and meal size for RYGB but not sham mice eating a meal 10 days ($r = 0.98$, $p < 0.0001$) but not 40 days ($r = 0.37$, n.s.) after surgery (Fig. 5a).

Analysis of double-labeled sections revealed a large percentage ($56.6 \pm 7\%$) of CGRP⁺ neurons expressing c-Fos after ingesting a meal in RYGB mice (Fig. 2e). Few double-labeled neurons were found in sham-operated mice eating a meal, or in RYGB and sham-operated mice that did not eat. There was a significant positive correlation between meal size and percent activated CGRP⁺ neurons in RYGB mice 10 days but not 40 days after surgery (Fig. 5b). These findings suggest that following an ad libitum meal, there is a significant increase in activity specifically in the CGRP⁺ subpopulation of neurons in the IPBN 10 days after RYGB.

To identify possible upstream and downstream neuronal populations, we also inspected the dorsal vagal complex and the CeA in the forebrain. There was strong meal-induced c-Fos

expression in the NTS and AP 10 days after RYGB compared to sham operation, with virtually no staining in fasted controls not eating a meal (Fig. 3a, b, c, g). Meal-induced c-Fos expression 40 days after RYGB surgery was less pronounced and not significantly different from sham or fasted controls (Fig. 3f, j). There was a moderate but not statistically significant positive correlation between meal size and c-Fos expression in the NTS in RYGB but not sham mice 10 days after surgery (Fig. 5c). Because TH-expressing catecholaminergic neurons in the NTS and AP have been strongly associated with satiation, we also carried out TH/c-Fos double-labeling in some animals sacrificed 10 days after surgery. While there was a significant increase in TH⁺ neurons expressing c-Fos in both NTS and AP in mice with RYGB compared with sham and fasted controls, we found very few double-labeled neurons, with less than 5% of all TH⁺ neurons activated (Fig. 3d, e, h, i).

As in the IPBN and NTS, there was significantly greater meal-induced c-Fos expression in the CeA 10 days after RYGB compared to sham surgery and no-meal conditions (Fig. 4a, b, d). c-Fos positive neurons were found in close proximity to intensely CGRP-immunoreactive fibers (Fig. 4c). Also similar to IPBN and NTS, this exaggerated c-Fos expression was much decreased 40 days after surgery, but unlike in the IPBN and NTS, it remained significantly higher than sham surgery and no meal controls (Fig. 4e). There was also a trend for a significant positive correlation between meal size and c-Fos expression in RYGB but not sham mice 10 days after surgery (Fig. 5d).

Discussion

Suppression of food intake is a key early ingredient of bariatric surgeries for rapid weight loss and improvement of glycemic control as shown by recent pair-feeding studies giving the same very low calorie diet typically eaten by bypass patients to non-surgical controls (12, 14). Surgery does not simply physically limit the amount of food eaten, as additional food deprivation (19), pregnancy (32), or pharmacological manipulation (18) results in drastic increases in daily food intake and body weight in rat models of sleeve gastrectomy and RYGB. If not simple physical restriction, what are the mechanisms reducing food intake after these surgeries? The present findings point to an important role of the brainstem anorexia pathway that was recently re-discovered in an impressive series of studies in mice (20–22, 28, 33).

Early suppression of food intake after RYGB may be mediated by activated CGRP neurons in the IPBN

Earlier literature has identified the PBN as a site of integration of viscerosensory information, including gastric distension and taste (34–36). There is an extensive literature demonstrating the activation of neurons in the PBN, particularly its lateral subnuclei following activation of viscerosensory input by electrical stimulation of vagal afferents (37), intraperitoneal administration of the satiety hormones CCK-8 (38), GLP-1 (39, 40), Exendin-4 (41), PYY (42), amylin (39, 43), the anorexigenic 5-HT reuptake inhibitor dexfenfluramine (38), systemic administration of LiCl (44, 45), and lipopolysaccharide(46). Importantly, a common effect of all these challenges is a reduction of food intake. Based on administration of small and large doses of CCK, Verbalis and colleagues had suggested long

ago that there is a continuum between satiation and nausea with an overlapping neural circuitry including the NTS and PBN (47). This view was reinforced by observations in ferrets with intravenous administration of CCK or LiCl (48) and discussed in a comprehensive recent review (49). Together, these findings suggest that under normal conditions, IPBN neurons are minimally activated, but that with large meals, more rapid ingestion, and other stimuli evoking mild to strong nausea and malaise, activation becomes stronger (50, 51).

More recently, it was demonstrated that the number of c-Fos-activated CGRP⁺ neurons in the IPBN of mice was positively correlated with the magnitude of food intake suppression across conditions including CCK, lithium chloride and lipopolysaccharide administration, as well as ablation of hypothalamic AGRP⁺ neurons (28). Most importantly, food intake was acutely suppressed by selective optogenetic stimulation of CGRP⁺ neurons in the IPBN that project to the amygdala, and selective pharmacogenetic stimulation extended over a period of 4 days led to potent and sustained suppression of food intake and an approximately 15% loss of body weight (28).

Our findings suggest that these same CGRP⁺ neurons are activated as a consequence of food ingestion during the early postsurgical period following RYGB. However, it is unclear whether or not this is due to increased stimulation, or decreased inhibition by AGRP⁺ neurons in the arcuate nucleus. In arcuate AGRP⁺ neuron ablation studies, it was shown that suppression of arcuate nucleus AGRP⁺ neuronal activity leads to hyperactivity of IPBN CGRP⁺ neurons (20). Our data shows that there is no significant increase in IPBN activity in the fasted state, suggesting that there is no chronic decrease in inhibition by arcuate AGRP⁺ neurons. To directly test the hypothesis that hyperactivity of CGRP neurons in the IPBN is responsible for the early suppression of food intake after RYGB, transgenic mouse models allowing selective silencing of CGRP neurons (28) will be necessary.

Exaggerated c-Fos expression in the NTS, AP, and amygdala defines a larger brainstem anorexia pathway

There is a large body of literature demonstrating neural activation of NTS neurons by stimuli that are associated with eating a meal [see (49) for review]. Here, we show that eating a voluntary meal produces a much larger neuronal activation in the NTS and AP in mice 10 days after RYGB surgery compared with sham surgery. Somewhat unexpectedly, the meal induced c-Fos response was very small or absent in sham mice. This could be due to the high-fat feeding regimen, known to attenuate vagal afferent satiety signaling (52).

Exaggerated activation of NTS neurons in RYGB mice is likely caused by signals originating from the rearranged gut as a consequence of food ingestion during the early postsurgical period. However, it is unclear what signals are required for this response. It has been speculated that exaggerated postprandial levels of the anorexic gut hormones GLP-1 and PYY, routinely seen after RYGB and VSG in humans (53, 54), are responsible for suppression of food intake. However, recent studies in GLP-1 receptor-deficient mice do not support such a role for GLP-1 (31, 55, 56). Alternatively, signals generated by food in the gut could reach the NTS via stimulation by the sensory vagus nerve. Vagal afferent nerve terminals innervating the small intestine are sensitive to both mechanical and chemical

stimuli and are thought to be important for meal termination and meal size (57). At least some of these afferents are left intact by both RYGB and VSG, and their intentional transection at the time of surgery results in attenuated weight loss (58, 59). A human study demonstrated that higher intra-luminal pressure in the Roux limb following RYGB is correlated with smaller meal size (60). Together, these findings suggest that after RYGB, the largely undigested food reaching the Roux limb excessively stimulates vagal nerve endings leading to exaggerated activation of the NTS → IPBN → CeA pathway.

A role for the CeA in suppression of food intake also begins to emerge. CeA PKC- δ^+ neurons in particular have been shown to be innervated directly by anorexigenic IPBN CGRP $^+$ neurons, and their activity is necessary for the suppression of food intake by CCK, bitter taste, and natural satiation (61). Consistent with these findings, our data show significantly increased activation of CeA neurons induced by a voluntary meal, 10 days after RYGB. The activated neurons were in close proximity to CGRP-positive fibers, further suggesting that they are direct downstream targets of CGRP neurons in the IPBN. Using the same antibody as Cai et al. (61), we were unable to positively identify these activated neurons as PKC- δ^+ , but the location and distribution was identical, suggesting that CeA PKC- δ^+ neurons downstream of IPBN CGRP $^+$ neurons play a key role in suppressing food intake in the early postsurgical period after RYGB. However, the neural circuits downstream of CeA PKC- δ^+ neurons are currently unclear. CeA PKC- δ^+ neurons make extensive intra-amygdalar connections, and GABA signaling within the amygdala is required for CeA PKC- δ^+ neurons to elicit their anorexigenic effects (61). However, the identity of the CeA output neurons and their projections to other brain areas are not known. Because most CeA neurons are GABAergic (62), it has been suggested that they may exert their influence by inhibiting areas responsible for increasing food intake, such as the lateral hypothalamus or the arcuate nucleus (24).

Absence of meal-induced exaggerated c-Fos later after RYGB suggests adaptive mechanisms

We found that exaggerated signaling through the NTS → IPBN → CeA pathway is no longer, or only weakly, present at 40 days after RYGB surgery. There are several interpretations for this adaptation. First, the slightly but significantly smaller meal size of RYGB mice at 40 days compared to 10 days could have contributed to the diminished neural activation. However, the difference was small (-29%) and unlikely explains the much larger decrease (-75%) in IPBN c-Fos expression. More importantly, there was a strong positive correlation between meal size and IPBN c-Fos expression as well as between meal size and percent CGRP $^+$ neuron activation in RYGB mice 10 but not 40 days after surgery.

Second, it is possible that the gastrointestinal consequences of eating a meal are no longer aversive and do not lead to increased vagal afferent activity. This conclusion is supported by the lack of correlation between meal size and c-Fos activation throughout the NTS → IPBN → CeA pathway 40 days after surgery. It is also indirectly supported by the observation that the Roux and common limbs adapt to the unhindered delivery of undigested food by growing in thickness and diameter after RYGB in rats (63, 64).

Third, because mice had slightly but significantly shifted preference towards chow at 40 days after surgery, providing only high-fat for the test meal could have caused an aversive response, leading to a stronger activation of the brainstem anorexia pathway. However, showing only small and non-significant activation at 40 days in the face of significant activation at 10 days, when there was no shift in preference, does not support this argument.

The most plausible explanation is that meals no longer activate c-Fos in the anorexia pathway 40 days after surgery because of behavioral adaptation towards smaller meal size. Studies in rats (29) and humans (17) have demonstrated that meal size is drastically reduced after RYGB surgery, and when food intake of RYGB rats is increased by pharmacological manipulation, they increase meal frequency but not meal size (18). RYGB patients are known to go through a learning process in which meal size and eating rate are gradually reduced to make individual eating episodes less aversive (17). Similarly, we have observed that rats and mice often show large fluctuations in food intake from one day to another, suggesting that eating too much on one day triggers an aversive response reducing intake on the next day (unpublished observations). In this study, we have not systematically assessed meal parameters under ad libitum conditions. However, the voluntary meal ingested after 16 h food deprivation was clearly smaller and slower in RYGB compared with sham mice at both time points (forcing us to prematurely stop the meal in sham mice). The fact that meal size in RYGB mice was lower 40 days compared with 10 days after surgery suggests that the behavioral adaptation to smaller meal size was not complete 10 days after surgery. The molecular mechanism for this behavioral adaptation could potentially involve synaptic plasticity within the anorexia pathway. It has been shown that repeated systemic administration of LiCl reduces expression of NR2B subunits of NMDA receptors in IPBN neurons, resulting in suppression of neuronal excitability (33). Because changes in subunit composition of NMDA receptors are known to contribute to synaptic plasticity(65), exaggerated signaling through this pathway early after surgery may lead to adaptive behavioral changes.

It is interesting to speculate that exaggerated activation of the brainstem anorexia pathway is linked to a changed body weight set point. We have previously provided behavioral evidence for a changed set point after RYGB in rats and mice (18)(Hao et al., *Obesity*, in press), although the molecular mechanisms underlying this phenomenon are not well understood. The idea that once the set point is changed, a hyperactive anorexia pathway is no longer required is intriguing and demands further testing.

We cannot exclude weight loss per se as a factor for the higher meal-induced activation of the anorexia pathway in RYGB vs. Sham mice. This could only be tested with a weight-matched control group. However, given that anorexia pathway activation was very different in the face of similar weight loss at 10 and 40 days, this explanation is less likely.

In conclusion, we find increased signaling through the potent anorexigenic NTS → IPBN → CeA pathway in the early postoperative period of RYGB surgery in the mouse. The consequences of this hyperactivation may be twofold. First, it is likely responsible for the strong early suppression of food intake after RYGB, known to be mainly responsible for the early improvements in glycemic control in humans. Second, hyperactivity of this pathway

may play an important role in changing eating behavior towards smaller and slower meals, resulting in some of the longer-term beneficial effects.

Acknowledgments

Support: This work was supported by National Institutes of Health grants DK047348 (HRB), DK068036 (JY), and DK092587 (HM).

We thank Neelima Gonugunta for help with immunohistochemistry. Supported by the National Institutes of Health grants DK047348 (HRB), DK085495 (JY), and DK092587 (HM).

References

1. Flynn CR, Albaugh VL, Cai S, Cheung-Flynn J, Williams PE, Brucker RM, et al. Bile diversion to the distal small intestine has comparable metabolic benefits to bariatric surgery. *Nat Commun*. 2015; 6:7715. [PubMed: 26197299]
2. Ryan KK, Tremaroli V, Clemmensen C, Kovatcheva-Datchary P, Myronovych A, Karns R, et al. FXR is a molecular target for the effects of vertical sleeve gastrectomy. *Nature*. 2014; 509:183–188. [PubMed: 24670636]
3. Liou AP, Paziuk M, Luevano JM Jr, Machineni S, Turnbaugh PJ, Kaplan LM. Conserved shifts in the gut microbiota due to gastric bypass reduce host weight and adiposity. *Sci Transl Med*. 2013; 5:178ra141.
4. Zechner JF, Mirshahi UL, Satapati S, Berglund ED, Rossi J, Scott MM, et al. Weight-independent effects of roux-en-Y gastric bypass on glucose homeostasis via melanocortin-4 receptors in mice and humans. *Gastroenterology*. 2013; 144:580–590. e587. [PubMed: 23159449]
5. Saeidi N, Meoli L, Nestoridi E, Gupta NK, Kvas S, Kucharczyk J, et al. Reprogramming of intestinal glucose metabolism and glycemic control in rats after gastric bypass. *Science*. 2013; 341:406–410. [PubMed: 23888041]
6. Shin AC, Zheng H, Pistell PJ, Berthoud HR. Roux-en-Y gastric bypass surgery changes food reward in rats. *Int J Obes (Lond)*. 2011; 35:642–651. [PubMed: 20805826]
7. Chandarana K, Gelegen C, Karra E, Choudhury AI, Drew ME, Fauveau V, et al. Diet and gastrointestinal bypass-induced weight loss: the roles of ghrelin and peptide YY. *Diabetes*. 2011; 60:810–818. [PubMed: 21292870]
8. Mul JD, Begg DP, Alsters SI, van Haaften G, Duran KJ, D'Alessio DA, et al. Effect of vertical sleeve gastrectomy in melanocortin receptor 4-deficient rats. *Am J Physiol Endocrinol Metab*. 2012; 303:E103–110. [PubMed: 22535749]
9. Chambers AP, Jessen L, Ryan KK, Sisley S, Wilson-Perez HE, Stefater MA, et al. Weight-independent changes in blood glucose homeostasis after gastric bypass or vertical sleeve gastrectomy in rats. *Gastroenterology*. 2011; 141:950–958. [PubMed: 21699789]
10. Hatoum IJ, Stylopoulos N, Vanhoose AM, Boyd KL, Yin DP, Ellacott KL, et al. Melanocortin-4 Receptor Signaling Is Required for Weight Loss after Gastric Bypass Surgery. *J Clin Endocrinol Metab*. 2012
11. le Roux CW, Welbourn R, Werling M, Osborne A, Kokkinos A, Laurenus A, et al. Gut hormones as mediators of appetite and weight loss after Roux-en-Y gastric bypass. *Ann Surg*. 2007; 246:780–785. [PubMed: 17968169]
12. Lingvay I, Guth E, Islam A, Livingston E. Rapid Improvement of Diabetes After Gastric Bypass Surgery: Is It the Diet or Surgery? *Diabetes Care*. 2013
13. Lips MA, de Groot GH, van Klinken JB, Aarts E, Berends FJ, Janssen IM, et al. Calorie Restriction is a Major Determinant of the Short-Term Metabolic Effects of Gastric Bypass Surgery in Obese Type 2 Diabetic Patients. *Clin Endocrinol (Oxf)*. 2013
14. Jackness C, Karmally W, Febres G, Conwell IM, Ahmed L, Bessler M, et al. Very Low Calorie Diet Mimics the Early Beneficial Effect of Roux-en-Y Gastric Bypass on Insulin Sensitivity and Beta-Cell Function in Type 2 Diabetic Patients. *Diabetes*. 2013

15. Schmidt JB, Pedersen SD, Gregersen NT, Vestergaard L, Nielsen MS, Ritz C, et al. Effects of RYGB on energy expenditure, appetite and glycemic control: a randomized controlled clinical trial. *Int J Obes (Lond)*. 2015
16. Sjostrom L, Lindroos AK, Peltonen M, Torgerson J, Bouchard C, Carlsson B, et al. Lifestyle, diabetes, and cardiovascular risk factors 10 years after bariatric surgery. *N Engl J Med*. 2004; 351:2683–2693. [PubMed: 15616203]
17. Laurenius A, Larsson I, Bueter M, Melanson KJ, Bosaeus I, Forslund HB, et al. Changes in eating behaviour and meal pattern following Roux-en-Y gastric bypass. *Int J Obes (Lond)*. 2012; 36:348–355. [PubMed: 22124454]
18. Mumphrey MB, Hao Z, Townsend RL, Patterson LM, Morrison CD, Munzberg H, et al. Reversible hyperphagia and obesity in rats with gastric bypass by central MC3/4R blockade. *Obesity (Silver Spring)*. 2014
19. Stefater MA, Perez-Tilve D, Chambers AP, Wilson-Perez HE, Sandoval DA, Berger J, et al. Sleeve gastrectomy induces loss of weight and fat mass in obese rats, but does not affect leptin sensitivity. *Gastroenterology*. 2010; 138:2426–2436. 2436 e2421–2423. [PubMed: 20226189]
20. Wu Q, Boyle MP, Palmiter RD. Loss of GABAergic signaling by AgRP neurons to the parabrachial nucleus leads to starvation. *Cell*. 2009; 137:1225–1234. [PubMed: 19563755]
21. Wu Q, Clark MS, Palmiter RD. Deciphering a neuronal circuit that mediates appetite. *Nature*. 2012; 483:594–597. [PubMed: 22419158]
22. Wu Q, Palmiter RD. GABAergic signaling by AgRP neurons prevents anorexia via a melanocortin-independent mechanism. *Eur J Pharmacol*. 2010
23. Atasoy D, Betley JN, Su HH, Sternson SM. Deconstruction of a neural circuit for hunger. *Nature*. 2012; 488:172–177. [PubMed: 22801496]
24. Sternson SM. Hypothalamic survival circuits: blueprints for purposive behaviors. *Neuron*. 2013; 77:810–824. [PubMed: 23473313]
25. Dobolyi A, Irwin S, Makara G, Usdin TB, Palkovits M. Calcitonin gene-related peptide-containing pathways in the rat forebrain. *J Comp Neurol*. 2005; 489:92–119. [PubMed: 15977170]
26. D'Hanis W, Linke R, Yilmazer-Hanke DM. Topography of thalamic and parabrachial calcitonin gene-related peptide (CGRP) immunoreactive neurons projecting to subnuclei of the amygdala and extended amygdala. *J Comp Neurol*. 2007; 505:268–291. [PubMed: 17879271]
27. Schwaber JS, Sternini C, Brecha NC, Rogers WT, Card JP. Neurons containing calcitonin gene-related peptide in the parabrachial nucleus project to the central nucleus of the amygdala. *J Comp Neurol*. 1988; 270:416–426. 398–419. [PubMed: 2836477]
28. Carter ME, Soden ME, Zweifel LS, Palmiter RD. Genetic identification of a neural circuit that suppresses appetite. *Nature*. 2013; 503:111–114. [PubMed: 24121436]
29. Zheng H, Shin AC, Lenard NR, Townsend RL, Patterson LM, Sigalet DL, et al. Meal patterns, satiety, and food choice in a rat model of Roux-en-Y gastric bypass surgery. *Am J Physiol Regul Integr Comp Physiol*. 2009; 297:R1273–1282. [PubMed: 19726714]
30. Hao Z, Zhao Z, Berthoud HR, Ye J. Development and verification of a mouse model for roux-en-Y gastric bypass surgery with a small gastric pouch. *PLoS ONE*. 2013; 8:e52922. [PubMed: 23326365]
31. Ye J, Hao Z, Mumphrey MB, Townsend RL, Patterson LM, Stylopoulos N, et al. GLP-1 receptor signaling is not required for reduced body weight after RYGB in rodents. *Am J Physiol Regul Integr Comp Physiol*. 2014; 306:R352–362. [PubMed: 24430883]
32. Grayson BE, Schneider KM, Woods SC, Seeley RJ. Improved rodent maternal metabolism but reduced intrauterine growth after vertical sleeve gastrectomy. *Sci Transl Med*. 2013; 5:199ra112.
33. Wu Q, Zheng R, Srisai D, McNight GS, Palmiter RD. The NR2B subunit of the NMDA glutamate receptor in the parabrachial nucleus regulates appetite. *PNAS*. 2013 In Press.
34. Baird JP, Travers JB, Travers SP. Parametric analysis of gastric distension responses in the parabrachial nucleus. *Am J Physiol Regul Integr Comp Physiol*. 2001; 281:R1568–1580. [PubMed: 11641130]
35. Baird JP, Travers SP, Travers JB. Integration of gastric distension and gustatory responses in the parabrachial nucleus. *Am J Physiol Regul Integr Comp Physiol*. 2001; 281:R1581–1593. [PubMed: 11641131]

36. Karimnamazi H, Travers SP, Travers JB. Oral and gastric input to the parabrachial nucleus of the rat. *Brain Res.* 2002; 957:193–206. [PubMed: 12445962]
37. Gieroba ZJ, Blessing WW. Fos-containing neurons in medulla and pons after unilateral stimulation of the afferent abdominal vagus in conscious rabbits. *Neuroscience.* 1994; 59:851–858. [PubMed: 7914681]
38. Li BH, Rowland NE. Effects of vagotomy on cholecystokinin- and dexfenfluramine-induced Fos-like immunoreactivity in the rat brain. *Brain Res Bull.* 1995; 37:589–593. [PubMed: 7670882]
39. Rowland NE, Crews EC, Gentry RM. Comparison of Fos induced in rat brain by GLP-1 and amylin. *Regul Pept.* 1997; 71:171–174. [PubMed: 9350975]
40. Degen L, Oesch S, Casanova M, Graf S, Ketterer S, Drewe J, et al. Effect of peptide YY3–36 on food intake in humans. *Gastroenterology.* 2005; 129:1430–1436. [PubMed: 16285944]
41. Labouesse MA, Stadlbauer U, Weber E, Arnold M, Langhans W, Pacheco-Lopez G. Vagal afferents mediate early satiation and prevent flavour avoidance learning in response to intraperitoneally infused exendin-4. *J Neuroendocrinol.* 2012; 24:1505–1516. [PubMed: 22827554]
42. Baraboi ED, Michel C, Smith P, Thibodeau K, Ferguson AV, Richard D. Effects of albumin-conjugated PYY on food intake: the respective roles of the circumventricular organs and vagus nerve. *Eur J Neurosci.* 2010; 32:826–839. [PubMed: 20646064]
43. Lutz TA. Pancreatic amylin as a centrally acting satiating hormone. *Curr Drug Targets.* 2005; 6:181–189. [PubMed: 15777188]
44. Lamprecht R, Dudai Y. Differential modulation of brain immediate early genes by intraperitoneal LiCl. *Neuroreport.* 1995; 7:289–293. [PubMed: 8742472]
45. Swank MW, Bernstein IL. c-Fos induction in response to a conditioned stimulus after single trial taste aversion learning. *Brain Res.* 1994; 636:202–208. [PubMed: 8012803]
46. Gaykema RP, Daniels TE, Shapiro NJ, Thacker GC, Park SM, Goehler LE. Immune challenge and satiety-related activation of both distinct and overlapping neuronal populations in the brainstem indicate parallel pathways for viscerosensory signaling. *Brain Res.* 2009; 1294:61–79. [PubMed: 19646973]
47. Verbalis JG, McCann MJ, McHale CM, Stricker EM. Oxytocin secretion in response to cholecystokinin and food: differentiation of nausea from satiety. *Science.* 1986; 232:1417–1419. [PubMed: 3715453]
48. Billig I, Yates BJ, Rinaman L. Plasma hormone levels and central c-Fos expression in ferrets after systemic administration of cholecystokinin. *Am J Physiol Regul Integr Comp Physiol.* 2001; 281:R1243–1255. [PubMed: 11557633]
49. Maniscalco JW, Kreisler AD, Rinaman L. Satiation and stress-induced hypophagia: examining the role of hindbrain neurons expressing prolactin-releasing Peptide or glucagon-like Peptide 1. *Front Neurosci.* 2012; 6:199. [PubMed: 23346044]
50. Emond M, Schwartz GJ, Moran TH. Meal-related stimuli differentially induce c-Fos activation in the nucleus of the solitary tract. *Am J Physiol Regul Integr Comp Physiol.* 2001; 280:R1315–1321. [PubMed: 11294749]
51. Kreisler AD, Davis EA, Rinaman L. Differential activation of chemically identified neurons in the caudal nucleus of the solitary tract in non-entrained rats after intake of satiating vs. non-satiating meals. *Physiol Behav.* 2014; 136:47–54. [PubMed: 24508750]
52. de Lartigue G, Ronveaux CC, Raybould HE. Vagal plasticity the key to obesity. *Mol Metab.* 2014; 3:855–856. [PubMed: 25506551]
53. Peterli R, Steinert RE, Woelnerhanssen B, Peters T, Christoffel-Courtin C, Gass M, et al. Metabolic and hormonal changes after laparoscopic Roux-en-Y gastric bypass and sleeve gastrectomy: a randomized, prospective trial. *Obes Surg.* 2012; 22:740–748. [PubMed: 22354457]
54. le Roux CW, Aylwin SJ, Batterham RL, Borg CM, Coyle F, Prasad V, et al. Gut hormone profiles following bariatric surgery favor an anorectic state, facilitate weight loss, and improve metabolic parameters. *Ann Surg.* 2006; 243:108–114. [PubMed: 16371744]
55. Mokadem M, Zechner JF, Margolskee RF, Drucker DJ, Aguirre V. Effects of Roux-en-Y gastric bypass on energy and glucose homeostasis are preserved in two mouse models of functional glucagon-like peptide-1 deficiency. *Mol Metab.* 2014; 3:191–201. [PubMed: 24634822]

56. Wilson-Perez HE, Chambers AP, Ryan KK, Li B, Sandoval DA, Stoffers D, et al. Vertical sleeve gastrectomy is effective in two genetic mouse models of glucagon-like Peptide 1 receptor deficiency. *Diabetes*. 2013; 62:2380–2385. [PubMed: 23434938]
57. Powley TL, Phillips RJ. Gastric satiation is volumetric, intestinal satiation is nutritive. *Physiol Behav*. 2004; 82:69–74. [PubMed: 15234593]
58. Bueter M, Lowenstein C, Ashrafian H, Hillebrand J, Bloom SR, Olbers T, et al. Vagal sparing surgical technique but not stoma size affects body weight loss in rodent model of gastric bypass. *Obes Surg*. 2010; 20:616–622. [PubMed: 20119735]
59. Hao Z, Townsend RL, Mumphrey MB, Patterson LM, Ye J, Berthoud HR. Vagal innervation of intestine contributes to weight loss After Roux-en-Y gastric bypass surgery in rats. *Obes Surg*. 2014; 24:2145–2151. [PubMed: 24972684]
60. Bjorklund P, Laurenus A, Een E, Olbers T, Lonroth H, Fandriks L. Is the roux limb a determinant for meal size after gastric bypass surgery? *Obes Surg*. 2010; 20:1408–1414. [PubMed: 20517654]
61. Cai H, Haubensak W, Anthony TE, Anderson DJ. Central amygdala PKC-delta(+) neurons mediate the influence of multiple anorexigenic signals. *Nat Neurosci*. 2014; 17:1240–1248. [PubMed: 25064852]
62. Haubensak W, Kunwar PS, Cai H, Ciochi S, Wall NR, Ponnusamy R, et al. Genetic dissection of an amygdala microcircuit that gates conditioned fear. *Nature*. 2010; 468:270–276. [PubMed: 21068836]
63. Mumphrey MB, Patterson LM, Zheng H, Berthoud HR. Roux-en-Y gastric bypass surgery increases number but not density of CCK-, GLP-1-, 5-HT-, and neurotensin-expressing enteroendocrine cells in rats. *Neurogastroenterol Motil*. 2013; 25:e70–79. [PubMed: 23095091]
64. Hansen CF, Bueter M, Theis N, Lutz T, Paulsen S, Dalboge LS, et al. Hypertrophy Dependent Doubling of L-Cells in Roux-en-Y Gastric Bypass Operated Rats. *PLoS ONE*. 2013; 8:e65696. [PubMed: 23776529]
65. Yashiro K, Philpot BD. Regulation of NMDA receptor subunit expression and its implications for LTD, LTP, and metaplasticity. *Neuropharmacology*. 2008; 55:1081–1094. [PubMed: 18755202]

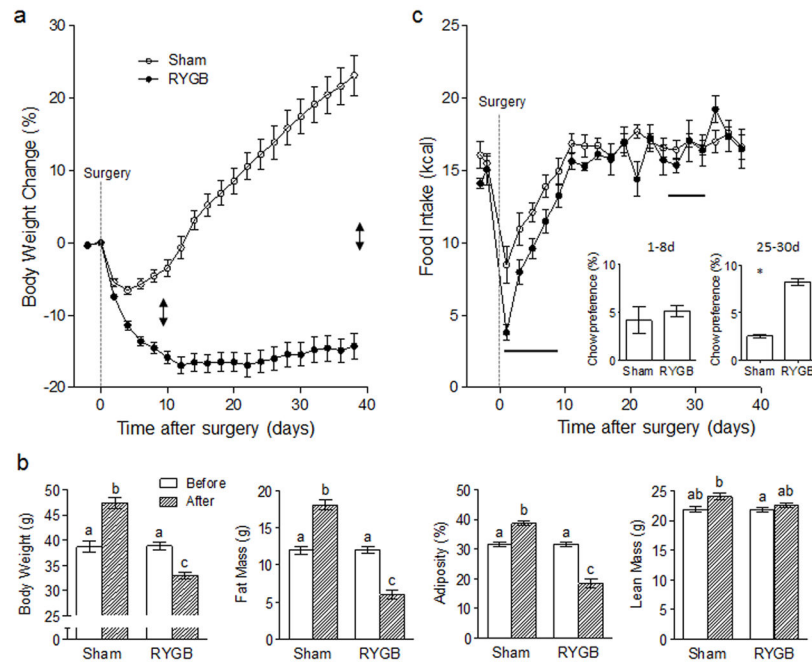


Fig. 1. Effects of Roux-en-Y gastric bypass surgery on body weight (a), body composition (b), and food intake (c) in mice made obese by exposure for 14 weeks to a two-choice diet consisting of high-fat and regular (low-fat) chow. **a:** Change in body weight after RYGB (filled circles; $n = 39$ for days 1–8, $n = 15$ for days 10–40) or sham surgery (open circles; $n = 34$, 16) expressed in percent of pre-surgical body weight. Double arrows indicate the time of meal tests at 10 and 40 days after surgery. **b:** Body weight, absolute fat mass, relative fat mass (adiposity), and lean mass before and 40 days after RYGB ($n = 15$) or sham surgery ($n = 16$). Bars that do not share the same letters are significantly different from each other (based on ANOVA followed by Bonferroni-corrected multiple comparisons). **c:** Total food intake before and after RYGB (filled circles; $n = 28$ for days 1–8, $n = 4$ for days 10–36) or sham-surgery (open circles; $n = 24$, 7). The two horizontal bars mark periods during which chow preference (based on calories) was measured in both groups (data shown in inset). * $p < 0.05$, RYGB vs. Sham.

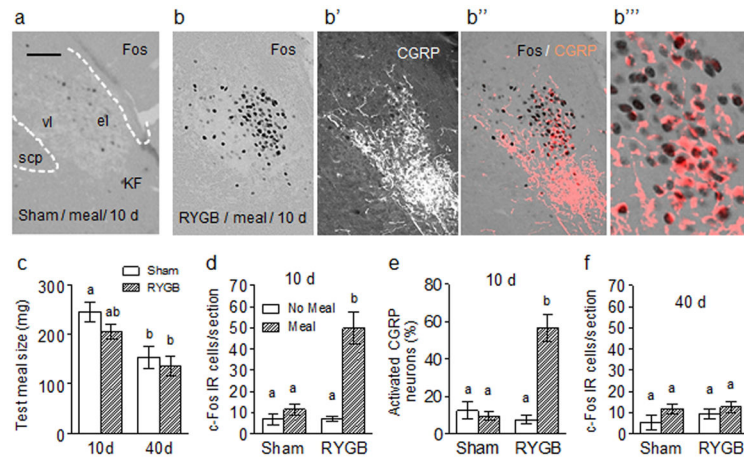


Fig. 2.

Meal-induced c-Fos expression in the lateral parabrachial nucleus of mice with RYGB or sham surgery. **a, b:** Representative micrographs showing c-Fos expression in the external lateral parabrachial nucleus in a mouse with sham-surgery (a) or RYGB (b) after consumption of a meal at 10 days after surgery. CGRP expression (b'), merged c-Fos (black) and CGRP (pink) expression (b''), as well as an enlarged detail of double-labeling (b''') are also shown for the RYGB mouse. **c:** High fat test meal size was not significantly different between RYGB and sham groups at either 10 or 40 days. **d,e:** Quantitative analysis of the number of c-Fos positive cells (d) and percent of CGRP positive cells expressing c-Fos (e) for meal consumption tests 10 days after surgery. **f:** Quantitative analysis of the number of c-Fos positive cells for meal consumption tests 40 days after surgery. Bars that do not share the same letters are significantly different from each other (based on ANOVA followed by Bonferroni-corrected multiple comparisons). Means \pm SEM of 5–10 mice. Scale bar in a: 100 μ m for a–b'' and 30 μ m for b'''. Abbreviations: el, external lateral subnucleus; KF, Kölliker-Fuse nucleus; scp, superior cerebellar peduncle; vl, ventrolateral subnucleus.

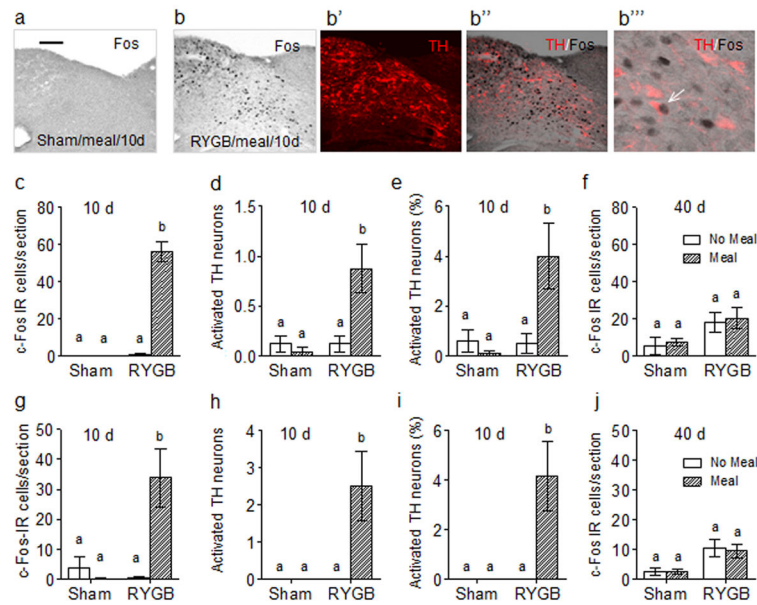


Fig. 3. Meal-induced c-Fos expression in the dorsal vagal complex of mice with RYGB or sham surgery. **a, b:** Representative micrographs showing c-Fos expression in the NTS and AP in a mouse with sham (a) or RYGB (b) surgery 10 days after surgery. TH expression (b') and merged c-Fos (black) and TH (pink) expression (b''), as well as an enlarged detail of double-labeling (b''') are also shown for the RYGB mouse (white arrow indicates lonely double-labelled neuron). **c-f:** Quantitative analysis of the number of c-Fos positive cells in the NTS 10 days (c) and 40 days (f) after surgery, as well as number (d) and percent (e) of TH neurons also expressing c-Fos for 10 day meal consumption tests. **g-j:** Quantitative analysis of the number of c-Fos positive cells in the area postrema 10 days (g) and 40 days (j) after surgery, as well as number (h) and percent (i) of TH neurons also expressing c-Fos for 10 day meal consumption tests. Means + SEM of 4–10 mice. Bars that do not share the same letters are significantly different from each other (based on ANOVA followed by Bonferroni-corrected multiple comparisons). Scale bar in a: 100 μm for a–b'' and 25 μm for b'''.

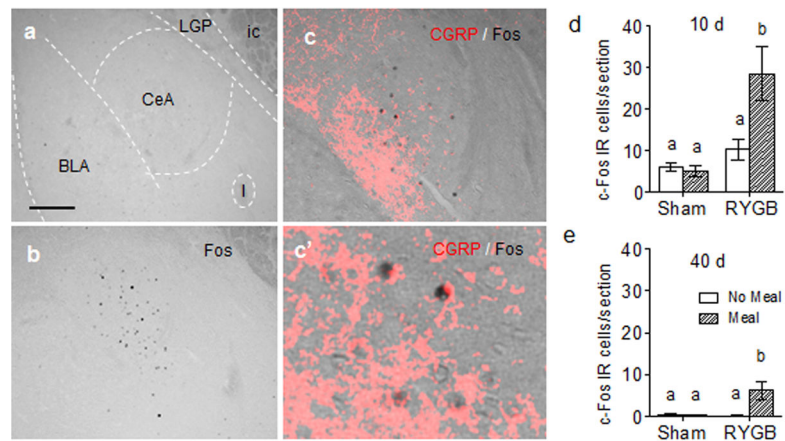


Fig. 4. Meal-induced c-Fos expression in the central nucleus of the amygdala (CeA) of mice with RYGB or sham surgery. **a, b:** Representative micrographs showing meal-induced c-Fos expression in the lateral part of CeA, 10 days after sham (a) or RYGB surgery (b). **c, c':** Low (c) and higher power (c') images of double-labeled section showing proximity of meal-induced c-fos (black) and CGRP-immunoreactive projections (pink) in CeA of mouse 10 days after RYGB. **d, e:** Quantitative analysis of meal-induced c-Fos expression in the CeA at 10 (d) and 40 (e) days after RYGB or sham surgery. Means + SEM of 4–8 mice. Bars that do not share the same letters are significantly different from each other (based on ANOVA followed by Bonferroni-corrected multiple comparisons). Scale bar in a: 100 μ m for a–c; 25 μ m for c'. Abbreviations: BLA, anterior basolateral amygdaloid nucleus; CeA, central amygdaloid nucleus; I, intercalated nuclei amygdala; ic, internal capsule; LGP, lateral globus pallidus.

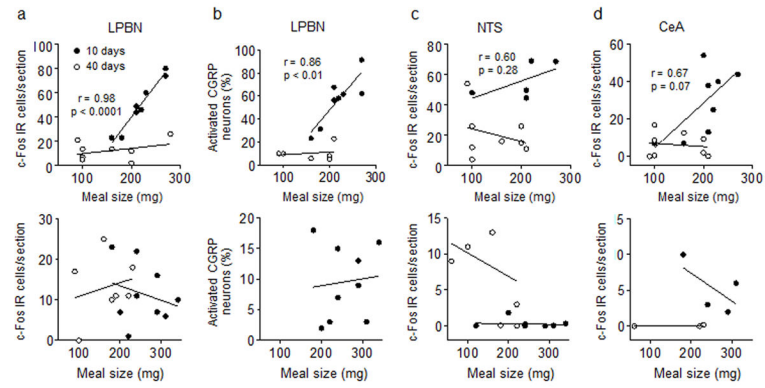


Fig. 5. Correlations between meal size and c-Fos expression in the IPBN (a,b), NTS (c), and CeA (d) of mice with RYGB ($n = 6-8$; upper panels) or sham surgery ($n = 3-9$; lower panels) 10 days after surgery. For the IPBN, the correlation between meal size and percent of activated CGRP⁺ neurons is also shown (b). All correlation coefficients and p values refer to meal tests 10 days after surgery. Correlations 40 days after surgery and in sham animals at both time points were weak and non-significant.